The Conformation of Apolipoprotein A-I in High-Density Lipoproteins Is Influenced by Core Lipid Composition and Particle Size: A Surface Plasmon Resonance Study†

Linda K. Curtiss,*,‡,§ David J. Bonnet,‡ and Kerry-Anne Rye‖

Departments of Immunology and Vascular Biology, The Scripps Research Institute, 10550 North Torrey Pines Road, La Jolla, California 92037, and Lipid Research Laboratory, Level 1, Hanson Centre, Frome Road, Adelaide, South Australia 5000

Received December 20, 1999; Revised Manuscript Received March 8, 2000

ABSTRACT: Plasma high-density lipoproteins (HDL) are a heterogeneous group of particles that vary in size as well as lipid and apoprotein composition. The effect of HDL core lipid composition and particle size on apolipoprotein (apo) A-I structure was studied using surface plasmon resonance (SPR) analysis of the binding of epitope-defined monoclonal antibodies. The association and dissociation rate constants of 12 unique apo A-I-specific monoclonal antibodies for isolated plasma HDL were calculated. In addition, the association rate constants of the antibodies were determined for homogeneous preparations of spherical reconstituted HDL (rHDL) that contained apo A-I as the sole apolipoprotein and differed either in their size or in their core lipid composition. This analysis showed that lipoprotein size affected the conformation of domains dispersed throughout the apo A-I molecule, but the conformation of the central domain between residues 121 and 165 was most consistently modified. In contrast, replacement of core cholesteryl esters with triglyceride in small HDL modified almost the entire molecule, with only two key N-terminal domains of apo A-I being unaffected. This finding suggested that the central and C-terminal domains of apo A-I are in direct contact with rHDL core lipids. This immunochemical analysis has provided valuable insight into how core lipid composition and particle size affect the structure of specific domains of apo A-I on HDL.

The high-density lipoproteins (HDL)[1] in human plasma consist of several subpopulations of predominantly spherical particles which are heterogeneous in size and composition. All spherical HDL have a hydrophobic core of cholesteryl esters (CE) and a small amount of triglyceride (TG) surrounded by a surface monolayer of phospholipids, unesterified cholesterol, and apolipoproteins *(1)*.

The precise conformation of apolipoprotein (apo) A-I, the major HDL apolipoprotein, is not known *(1)*. This is an issue of considerable importance as it may affect the function and cardioprotective properties of HDL *(2)*. Although physical−chemical approaches have revealed wide variations in the conformation of apo A-I on different plasma HDL subpopulations, there is no information about how core lipid composition or particle size affects the conformation of specific apo A-I domains. Plasma HDL cannot be used to investigate this issue because of the following: (i) they consist of multiple subpopulations of particles that vary widely in size and cannot be separated easily from each other; (ii) because of this heterogeneity, there is wide variation in the conformation of apo A-I between HDL subpopulations; (iii) in addition to apo A-I, HDL contain on their surface varying concentrations of other apolipoproteins (apo A-II, the C apolipoproteins, and apo E) as well as other plasma factors (such as paraoxonase, LCAT, and CETP) that can influence the conformation of apo A-I; and (iv) the core lipid composition of HDL varies according to diet and interactions with plasma factors *(3−5)*. These problems were overcome in the present study by using well-characterized preparations of spherical reconstituted HDL (rHDL) containing apo A-I as the only apolipoprotein and either cholesteryl esters or triglycerides as the sole core lipids *(6, 7)*. As the rHDL were homogeneous in size and composition, the conformation of apo A-I was uniform in each of the preparations.

Because apo A-I-specific monoclonal antibodies probe precise, defined regions (epitopes) of apo A-I *(8)*, studies of their reaction with homogeneous preparations of spherical rHDL, which differ only in size or core lipid composition, can provide important new structural information that cannot be obtained from the mixtures of particles that are present in plasma HDL. For example, studies of discoidal rHDL of varying size have suggested that there is considerable flexibility in the conformation of lipid-bound apo A-I *(2)*. If this is true, changes in the structure of specific domains of

† This work was supported by NIH Research Grant HL43815 to L.K.C. and by the National Health and Medical Research Council of Australia. K.-A.R. is a Senior Research Fellow of the National Heart Foundation of Australia.

* To whom correspondence should be addressed. Telephone: (858) 784-8248. FAX: (858) 784-9144. Email: lcurtiss@scripps.edu.

‡ Department of Immunology, The Scripps Research Institute.

§ Department of Vascular Biology, The Scripps Research Institute.

‖ Lipid Research Laboratory, Level 1.

[1] Abbreviations: HDL, high-density lipoprotein(s); SPR, surface plasmon resonance; rHDL, reconstituted HDL; apo, apolipoprotein; LCAT, lecithin cholesterol acyltransferase; CETP, cholesteryl ester transfer protein; CE, cholesteryl ester(s); TG, triglyceride(s); RU, response unit(s).

10.1021/bi992902m CCC: $19.00
Published on Web 04/19/2000

apo A-I in spherical HDL of different sizes may be observed as well.

Our immunochemical analysis of these homogeneous preparations of rHDL enabled us to directly assess the effects of particle size and core lipid composition on the conformation of defined domains of apo A-I. We used surface plasmon resonance (SPR) to measure the binding of a panel of epitope-defined, apo A-I-specific antibodies to plasma HDL and homogeneous preparations of rHDL. SPR detects changes in the effective refractive index integrated along an electromagnetic field that decays with distance from a thin metal surface containing immobilized protein, which in our case was an immobilized monoclonal antibody *(9−11)*. When fluid phase antigens such as HDL or purified reconstituted HDL (rHDL) flow over the sensor surface of the chip and are bound by antibody, the antigen/antibody reaction is monitored continuously and the association and disassociation phases visualized and integrated.

There are at least three distinct advantages of this system over existing enzyme-linked or radioimmunoassay systems. First, all molecular interactions are monitored by SPR in real time so that true association and disassociation rate constants rather than equilibrium constants are calculated. Second, none of the molecules, including the antibodies or HDL analytes, need to be tagged or labeled. Third, there is no need to know the starting concentration of the immobilized monoclonal antibody to assess how this antibody interacts with multiple forms of its cognate antigen *(9−11)*. Using this approach, we have shown that the apo A-I in spherical rHDL is very flexible and its conformation is regulated by the size and core lipid composition of the particles.

EXPERIMENTAL PROCEDURES

Plasma HDL for SPR Studies. HDL ($d = 1.063-1.21$ g/mL) were isolated from normal human plasma by standard ultracentrifugation techniques in the presence of protease inhibitors and antioxidants as described *(12)*. Donors were in all cases fasted, nonsmoking males. The plasma HDL was stored in 0.15 M NaCl containing 0.3 M EDTA and 1 mM Probucol at 4 °C, and filter-sterilized through a 0.22 μm filter immediately before use. Over the course of this study, three different preparations of HDL were studied.

Purification of CETP and LCAT. The LCAT and CETP were purified from pooled, human plasma as described *(7, 13)*. The LCAT generated 340 nmol of CE (mL of LCAT)$^{-1}$ h^{-1}. The activity of the CETP was 12.5 units/mL, where 1 unit is the transfer activity of 1 mL of pooled lipoprotein-deficient human plasma.

Preparation of rHDL. The rHDL were prepared in Adelaide, South Australia, and shipped on wet ice overnight to La Jolla, California, for analysis. Over a period of 6 months, three separate preparations were shipped and analyzed. LDL were isolated from pooled, human plasma by ultracentrifugation in the 1.019−1.055 g/mL density range and dialyzed against 0.01 M Tris-buffered saline (TBS) (pH 7.4) containing 0.15 M NaCl, 0.005% (w/v) EDTA-Na_2, and 0.006% (w/v) NaN_3. HDL were isolated from pooled, human plasma by ultracentrifugation in the 1.07−1.21 g/mL density range. Apo A-I was isolated from the HDL using standard procedures *(7)*.

Discoidal rHDL containing 1-palmitoyl-2-oleoylphosphatidylcholine (Sigma), unesterified cholesterol (Sigma), and apo A-I were prepared by cholate dialysis *(14)*. The discoidal rHDL were converted into large, spherical rHDL by incubation with LDL and LCAT as described *(7)*. The large, spherical rHDL contained only cholesteryl esters in their core and apo A-I as the sole apolipoprotein, (CE)rHDL.

Small, spherical (CE)rHDL were prepared by incubating the large spherical (CE)rHDL with CETP at 37 °C for 24 h *(15)*. When the incubation was complete, the small, spherical (CE)rHDL were isolated by ultracentrifugation in the 1.063−1.25 g/mL density range with a single spin at each of the lower and higher densities. Identical conditions were used for control incubations, where large, spherical (CE)rHDL were incubated with TBS without CETP.

Small, spherical rHDL containing triglycerides as the sole core lipid, (TG)rHDL, were prepared by incubating large, spherical (CE)rHDL with CETP and Intralipid (20% triglyceride, KabiVitrum AB, Stockholm, Sweden) *(7)*. When the incubation was complete, the small, spherical (TG)rHDL were isolated by ultracentrifugation in the 1.063−1.25 g/mL density range, with two spins at the lower density (to remove Intralipid) and a single spin at the upper density. The same conditions were used for control incubations of the starting large, spherical (CE)rHDL, Intralipid, and TBS.

All the rHDL were dialyzed extensively against TBS before use and were stored at 4 °C in the presence of 0.3 M EDTA-Na_2 and 1 mM Probucol. A Cobas Fara centrifugal analyzer was used to determine the concentrations of rHDL constituents. Particle sizes were determined by nondenaturing gradient gel electrophoresis *(13, 15)*. All of the (CE)- and (TG)rHDL were confirmed to contain only spherical particles using EM and to be free of lipid-free apo A-I using nondenaturing gradient gel electrophoresis and immunoblotting *(13, 15)*.

Monoclonal Antibodies. The monoclonal antibodies were described previously *(8, 12, 16−20)*. They were obtained from multiple fusions of spleens of immunized Balb/c mice with P3Ag8.653.1 myeloma cells using standard fusion protocols. The antibodies were purified from ascites by fast protein liquid chromatography on a Mono-Q HR 16/10 (100 mm × 16 mm i.d.) anion exchange column (Pharmacia), stored at −20 °C, and filtered through a 0.2 μm filter immediately before use.

Surface Plasmon Resonance Analysis. All SPR measurements were obtained on a BIAcore 2000 system (Pharmacia Biosensor AB, Uppsala, Sweden). The sensor chips were CM5 research grade. The immunosorbent-purified polyclonal rabbit anti-mouse Fc (RAMFc), surfactant P-20, and amine coupling kit were obtained from BIAcore, Inc.

Each apo A-I-specific antibody was bound to a CM5 chip by capture with RAMFc. Covalent attachment of the RAMFc onto the CM5 sensor chip was performed as previously described by Karlsson et al. *(9)*, with modification to immobilize RAMFc through all four flowcells simultaneously. PBS, pH 7.3, containing 0.005% surfactant P-20 (buffer) was filtered through a 0.2 μm filter and thoroughly degassed. A flow rate of 5 μL/min was used. The system temperature was 25 °C. The carboxymethylated dextran matrix in all four flowcells was activated simultaneously by injection of 40 μL of a mixture containing 37.5 mg of *N*-ethyl-*N*-(3-dimethylaminopropyl)carbodiimide (EDC)/mL and 5.75 mg of *N*-hydroxysuccinimide (NHS)/mL. RAMFc (75 μL of 30 μg/mL in 10 mM sodium acetate, pH 4.8) was

injected to bind to the activated sites followed by 70 μL of 1 M ethanolamine to block the remaining activated sites. Finally, 10 μL of 100 mM HCl was injected to remove noncovalently bound RAMFc. This coupling procedure resulted in the covalent attachment of 10 000−11 000 response units (RU) of RAMFc.

Following covalent attachment of the RAMFc, the individual purified monoclonal antibodies were injected and captured by the RAMFc. Buffer flow rate was 10 μL/min, and system temperature was 25 °C. Antibodies were diluted in buffer at protein concentrations between 1.9 and 10 μg/mL. The concentration of antibody needed to yield 400 RU of captured antibody was determined empirically using a 1 min injection of 10 μL of purified antibody. In these experiments, both control and specific antibodies were bound at approximately 400 RU. The resulting low surface binding capacity eliminated mass transport limitations *(21)*, as increased analyte flow rate had little effect on kinetic binding.

Analyte Binding Experiments. Data collection rate was set at 10 data points/s as recommended for kinetic experiments. A buffer flow rate of 10 μL/min and system temperature of 25 °C were used in all HDL binding experiments. The analytes (HDL or rHDL) were diluted in buffer. A typical experiment consisted of the generation of a single chip of immobilized RAMFc followed by the exposure of each flowcell to the same concentration of antibody. Then, a total of 0.04 mL of analyte (HDL or rHDL) was injected for 4 min with each flowcell receiving a different analyte concentration. To correct for the bulk refractive index effects observed with injection of the large molecular weight HDL or rHDL, control binding studies were performed with an irrelevant antibody. This was antibody G8C11, an IgG1 antibody that binds glucitollysine *(16)*. Following HDL association, dissociation was initiated by switching to buffer for an additional 1.5 min. After all flowcells were reacted and washed, they were regenerated with 20 μL of 100 mM HCl at 30 μL/min. After regeneration of the RAMFc-immobilized chip by 100 mM HCl, a slight drop in RU (approximately 10 RU per regeneration) occurred, which indicated complete removal of the antibody and analyte and/or loss of RAMFc from the chip surface.

Data Evaluation. Results were expressed in resonance response units, RU *(21)*. Data transformation and overlay plots were prepared with the BIAevaluation version 3.0 software. A control sensorgram, using the G8C11 antibody, which did not bind apo A-I plasma HDL or rHDL, was generated with each HDL or rHDL analyte concentration. Before evaluation, this background analyte association and dissociation control sensorgram was subtracted from the corresponding apo A-I-specific antibody/analyte binding sensorgram after first aligning the injection times and zeroing the baselines. The association and dissociation rate constants (k_a and k_d, respectively) were calculated from the individual association and dissociation phases. Where possible, the Langmuir model for 1:1 binding was used to solve simultaneously for k_a and k_d in which case the k_a and k_d fitting status was global and the R_{max} and RI fitting status was local *(22, 23)*. With each antigen preparation, three to four sensorgrams, each employing a different concentration of analyte, were evaluated globally for each apo A-I-specific antibody. If the Chi2 (χ^2) value indicated that the parameter values did not fit the data using global fitting, or if the residual plot and visual inspection of the data indicated a poor fit, then the Langmuir models for 1:1 association and for 1:1 dissociation were used to solve separately for k_a and k_d *(22, 23)*. In this case, the k_a and k_d fitting status was local. All HDL and rHDL analytes were run with each antibody on at least two different days. The calculated k_a's and k_d's in all cases represent the average of at least two complete and separate analyses. Multiple preparations of plasma HDL were analyzed and all analyses averaged to obtained the k_a's and k_d's shown in Table 1.

Pairwise Antibody Binding Experiments. Additional qualitative analyses were performed with pairs of competing and noncompeting antibodies. These studies were performed to determine if changes in the size or core lipid composition of the rHDL would alter the interaction of two different apo A-I-specific monoclonal antibodies that shared adjacent or proximal epitopes.

As described above, rabbit anti-mouse Fc (RAMFc) antibody was immobilized on a CM5 research grade chip as previously described, except each flowcell was reacted separately and a 10 μL activation volume was used. The yield of RAMFc was 3000−3500 RU per flowcell. The buffer was PBS containing 0.005% P20 surfactant, and the flow rate was 10 μL/min. The amount of rHDL captured was approximately 70 RU. This required adjusting the method parameters for each pair of antibodies. The capture antibody concentration range was 5−60 μg/mL, and the injection time ranged between 1 and 3 min. Nonspecific antibody (G8C11) was used to saturate RAMFc binding sites at a concentration of 100 μg/mL with a 10 min injection time. The rHDL particle molarity was 200−500 nM, and the injection time ranged between 4 and 19 min. To bind remaining apo A-I binding sites on the rHDL still exposed after capture, 3−4 μg/mL of the same capture antibody was injected over 1 min. The concentration range for the competing antibody was 1−20 μg/mL, and the injection time was 4 min. A set of four sensorgrams over a range of concentrations was obtained for each competing antibody as well as a corresponding set of control sensorgrams using the same concentrations of capture antibody. All data were evaluated with BIAevaluation 3.0 software. As before, the injection times were standardized, the baseline was averaged to zero, and a control sensorgram using capture antibody as the competing antibody was subtracted. The range of maximum RU per sensogram was between 200 and 500 RU. The sensorgram was fit to a 1:1 Langmuir association and dissociation model with global, but separate fitting as described *(21−23)*.

RESULTS

Binding of Monoclonal Antibody to Isolated Plasma HDL. Our complete panel of epitope-mapped human apo A-I-specific antibodies is illustrated on a linear model of apo A-I in Figure 1. The specific amino acid residues of each antibody are listed in Table 1. Also shown for each antibody in Table 1 are the following: (i) the inclusive amino acid residues of the assigned apo A-I epitopes; (ii) the Ig heavy chain class; and (iii) the concentration of purified monoclonal Ig that was injected to capture 400 RU of monoclonal Ig by the covalently immobilized RAMFc. This concentration was determined empirically for each individual antibody. Analysis of the individual RAMFc sensorgrams verified that 400 RU of each antibody including the control antibody G8C11 had been captured by the RAMFc.

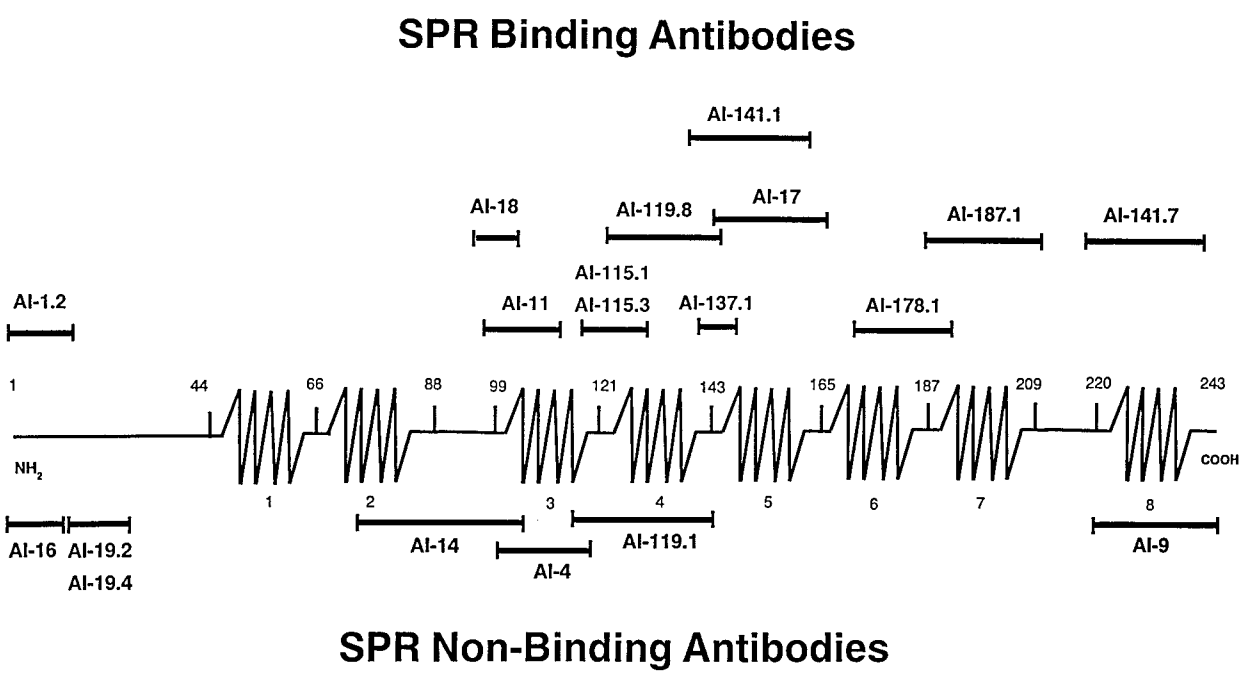

FIGURE 1: Linear representation of apo A-I showing the antibody-defined epitopes as broad horizontal lines above and below the linear model. Proline-punctuated β-turns are indicated by vertical lines and the α-helices by the wavy lines. Amino acid residues of the mature protein are indicated above the line, and the helices are numbered 1−8 below the line. Peptide binding assays used to map the epitopes on apo A-I have been published previously (*8*).

Table 1: Monoclonal Antibodies

antibody no.	epitope assignment (aa residues)	Ig class	Ig concn to yield 400 RU (μg/mL)	k_a for plasma HDL ($M^{-1}s^{-1}$)	k_d for plasma HDL (s^{-1})
AI-16	1−15	IgG2a	2.4	−[a]	−
AI-1.2	1−19	IgG2a	6.4	7.37×10^3	6.64×10^{-4}
AI-19.2	19−31	IgG1	6	−	−
AI-19.4	19−31	IgG2a	4.9	−	−
AI-14	74−105	IgG2a	3.1	−	−
AI-18	95−105	IgG1	3.2	3.33×10^3	3.81×10^{-3}
AI-11	96−111	IgG1	2.8	2.76×10^5	2.53×10^{-3}
AI-4	99−121	IgG1	1.9	−	−
AI-115.1	115−126	IgG1	3.7	1.68×10^4	3.84×10^{-3}
AI-115.3	115−126	IgG2a	3.7	6.70×10^3	4.86×10^{-3}
AI-119.1	119−144	IgG1	8.3	−	−
AI-119.8	119−144	IgG1	3.2	2.43×10^4	6.54×10^{-4}
AI-137.1	137−147	IgG1	5	4.68×10^4	8.17×10^{-4}
AI-141.1	141−164	IgG1	2.5	2.27×10^3	9.27×10^{-3}
AI-17	143−165	IgG1	3.5	8.24×10^5	1.20×10^{-3}
AI-178.1	178−200	IgG1	3.2	6.90×10^5	2.70×10^{-3}
AI-187.1	187−210	IgG	10	4.58×10^5	3.20×10^{-3}
AI-9	220−243	IgG1	3.4	−	−
AI-141.7	220−242	IgG1	4.5	2.52×10^5	4.35×10^{-4}
G8C11	glucitollysine	IgG1	3	−	−

[a] Could not be measured by SPR.

The binding of isolated plasma HDL to a single captured monoclonal antibody, AI-11, is shown in Figure 2A. The sensorgrams obtained with 10, 40, and 80 particle nM of plasma HDL are shown as solid lines. The interval between 125 and 350 s represented the rate of complex formation between antibody AI-11 and plasma HDL as the HDL flowed over the antibody immobilized on the metal surface. The dissociation or off phase was represented by the interval between 350 and 550 s as the sensor chips were washed with buffer containing no lipoprotein. Here, the sensorgram represented the fraction of the complexes that decayed. The Langmuir model for 1:1 binding that was used to calculate the association and dissociation rate constants is shown in closed circles and illustrates the closeness of fit between the real data and the model.

Each immobilized antibody listed in Table 1 was exposed to four different concentrations of plasma HDL. Listed are the mean association (k_a) and dissociation (k_d) rate constants measured on at least 2 separate days using at least three concentrations of fresh isolated plasma HDL (Table 1). Seven of the captured apo A-I-specific antibodies as well as the irrelevant control antibody (*16*) G8C11 showed no detectable binding to plasma HDL at concentrations up to 20 μM. Except for G8C11, specificity of these antibodies for human apo A-I has been demonstrated by Western blotting of SDS−PAGE gels *(17−20)*. However, there are many possible

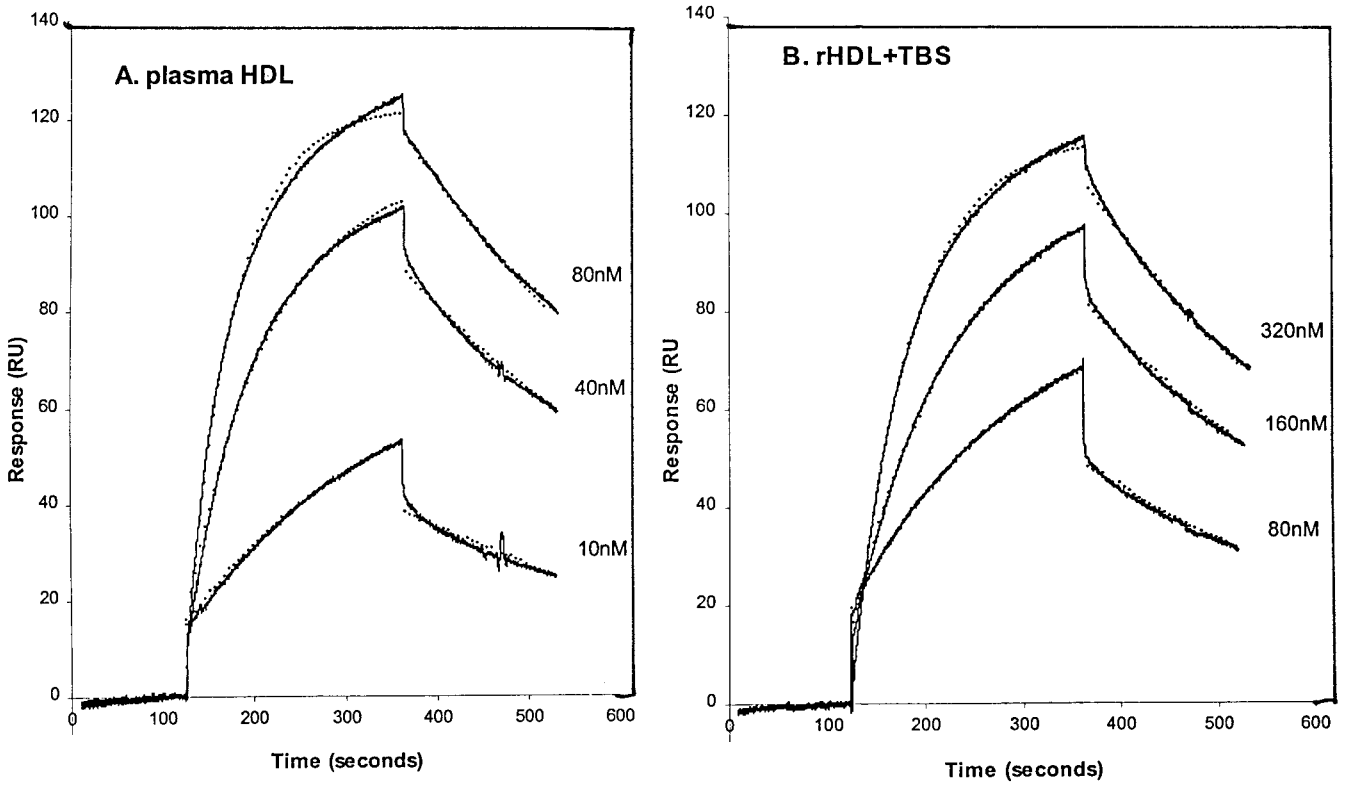

FIGURE 2: SPR sensorgrams for the real time association and dissociation of plasma HDL or rHDL to immobilized monoclonal antibody AI-11. Panel A: response units obtained with 10, 40, and 80 particle nM plasma HDL. Panel B: response units obtained with 80, 160, and 320 apo A-I nM of rHDL. The solid lines represent the sensorgram tracings, whereas the closed circles represent the Langmuir model for 1:1 binding that was used to calculate the plasma HDL k_a and k_d listed in Table 1 and the rHDL k_a and k_d shown in Figure 4.

reasons why binding was not observed with some of the antibodies, including: the nonbinding antibodies bind only free or denatured apo A-I, the binding of plasma HDL is not within the limits of detection, and the antibody only binds aged or oxidatively modified apo A-I or HDL. Moreover, it must be emphasized that plasma HDL is a heterogeneous population of particles and most monoclonal antibodies (even when they are present in excess) do not react with all apo A-I-containing plasma HDL (e.g., most apo A-I-specific antibodies are not pan HDL antibodies) *(17)*. Therefore, the preparation of isolated plasma HDL used in this study may not have contained sufficient amounts of a given reactive HDL subspecies.

Calculated k_a's for the 12 antibodies that did bind plasma HDL ranged from a high of 8.24×10^5 M^{-1} s^{-1} to a low of 2.27×10^3 M^{-1} s^{-1}, for antibodies AI-17 and AI-141.1, respectively. Interestingly, the epitopes of these two antibodies overlap a region between residues 143 and 165 of apo A-I (Figure 1), and the differing affinities are likely due to antibody preferences for different apo A-I conformations. Calculated k_d's for the same 12 antibodies ranged from 4.35×10^{-4} s^{-1} for the low dissociation (high avidity) antibody, AI-141.7, to 9.27×10^{-3} s^{-1} for the high dissociation (low avidity) antibody, AI-141.1. A comparison of the k_a and the k_d of each antibody for plasma HDL, as shown in Figure 3, confirmed that these two properties can, but need not be related. For example, antibody AI-141.1 had the lowest k_a and the highest k_d; antibody AI-17 had the highest k_a and a low k_d; whereas antibodies AI-119.8 and AI-1.2 had reasonably low k_a's as well as low k_d's for plasma HDL.

It is also important to note that antibody reactivity, affinity, and avidity were not related to antibody specificity. For

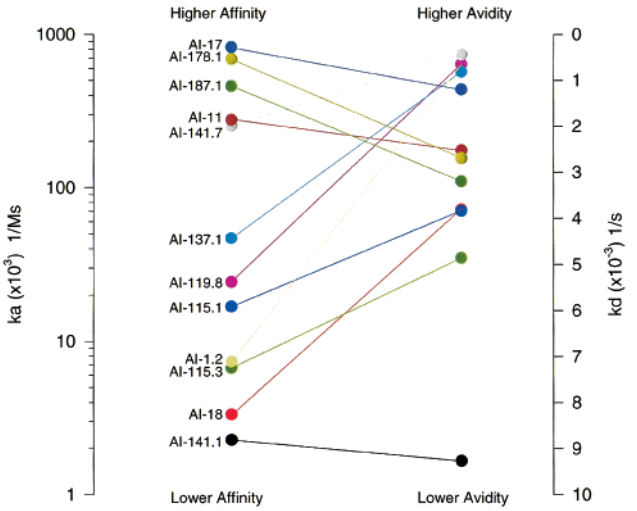

FIGURE 3: Relationship of the calculated plasma HDL k_a and k_d for each antibody. The k_a for each antibody is represented on a log scale on the left side, and the k_d for each antibody is represented on a linear scale on the right side. The scales are arbitrary and were chosen only to illustrate the rank order of these parameters for each antibody and to compare for each antibody the relationship between its k_a and k_d for isolated plasma HDL.

example, antibodies AI-1.2 and AI-16 both bound the N-terminal domain of apo A-I (Figure 1), yet antibody AI-16 showed no SPR-detectable reactivity for plasma HDL, whereas AI-1.2 did react (Table 1). Similarly, antibodies AI-115.5 and AI-115.3 bind to the same apo A-I epitope, yet had different affinities and avidities for this epitope on plasma HDL (Table 1). Therefore, as expected, neither antibody

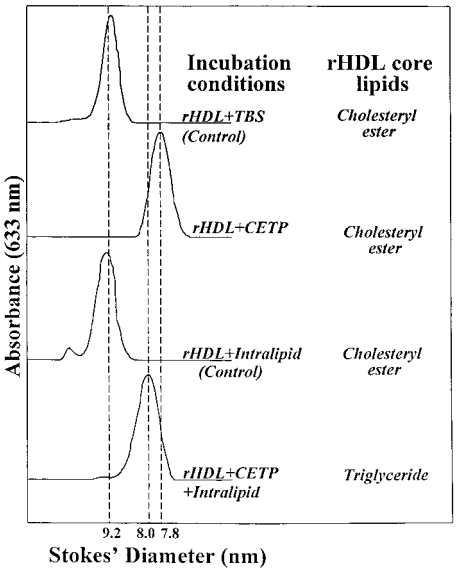

FIGURE 4: Particle size of rHDL. Small, spherical (CE)rHDL (diameter 7.8 nm) were prepared by incubating large, spherical (CE)rHDL (diameter 9.2 nm) (final apo A-I concentration 0.2 mg/mL) at 37 °C for 24 h in the presence of CETP (final activity 10.6 units/mL). Control incubations of large, spherical (CE)rHDL (final apo A-I concentration 0.2 mg/mL) and TBS also were carried out. The final volume of the incubations was 18.6 mL. At the end of the incubation, the small, spherical (CE)rHDL were isolated by ultracentrifugation as described under Experimental Procedures. Small, spherical (TG)rHDL (diameter 8.0 nm) were prepared by incubating the large, spherical (CE)rHDL (final apo A-I concentration 0.16 mg/mL) with Intralipid (final TG concentration 3.7 mg/mL) and CETP (final activity 5.5 units/mL) at 37 °C for 24 h. Identical conditions were used for control incubations of the large spherical (CE)rHDL with Intralipid and TBS. The final volume of the incubation mixtures was 22.4 mL. When the incubations were complete, the rHDL were isolated by ultracentrifugation as described under Experimental Procedures. The isolated rHDL were electrophoresed on a 3−35% nondenaturing gradient gel and stained with Coomassie Blue. Laser denitometric scans of the stained gel are shown.

affinity (k_a) nor antibody avidity (k_d) were defined by an antibody's specificity.

Characterization of rHDL. Large, spherical (CE)rHDL were prepared by incubating discoidal rHDL with LDL and LCAT. The large, spherical (CE)rHDL were 9.2 nm in diameter and contained apo A-I as their sole apoprotein and cholesteryl esters as the only core lipid (result not shown). Incubation at 37 °C for 24 h in the presence of TBS did not affect the size of the large, spherical (CE)rHDL (Figure 4). When the large, spherical (CE)rHDL were incubated at 37 °C for 24 h with CETP, they were converted into small, spherical (CE)rHDL, 7.8 nm in diameter.

The size of the large, spherical (CE)rHDL was not affected by incubation at 37 °C for 24 h with Intralipid. However, when they were incubated with Intralipid and CETP, small, spherical (TG)rHDL, which were 8.0 nm in diameter and contained triglycerides in their core, were formed (Figure 4). The stoichiometries of the control rHDL preparations and the rHDL which were incubated with CETP, or CETP and Intralipid, are shown in Table 2. The small amount of triglyceride in the control rHDL that were incubated with Intralipid probably reflected a trace amount of Intralipid remaining in the rHDL, rather than a spontaneous transfer of triglyceride from Intralipid to the rHDL *(7)*.

Table 2: Physical Properties of rHDL[a]

	PL/UC/CE/TG/AI[b] (mol/mol)	diameter[c] (nm)	MW[d] (Da)
rHDL	26.2/3.2/18.2/0.0/1.0	9.2	183906
rHDL+CETP	30.2/2.8/15.5/0.0/1.0	7.8	124860
rHDL+IL	29.9/1.0/18.5/0.5/1.0	9.2	190377
rHDL+CETP+IL	34.5/1.2/0.0/4.0/1.0	8	117055

[a] Spherical rHDL were incubated either alone or in the presence of CETP or in the presence of Intralipid alone or Intralipid and CETP as described in the legend to Figure 4. The concentrations of the individual constituents were determined as described (*7*). [b] PL, phospholipid; UC, unesterified cholesterol; CE, cholesteryl ester; A-I, apo A-I. [c] Determined by nondenaturing polyacrylamide gradient gel electrophoresis. [d] Calculated from the stoichiometry assuming that the control rHDL contained 3 molecules of apo A-I/particle (*7*) and the small rHDL, which were generated by incubation with CETP or CETP and Intralipid, contained 2 molecules of apo A-I/particle (*7*, *15*).

Binding of Monoclonal Antibody to rHDL. In contrast to the dissociation rate constant (k_d), the association rate constant is a dynamic measure of complex formation between an antibody and its apo A-I epitope on HDL. As such, the k_a is a measure of the closeness of fit between an antibody and its epitope. Moreover, because antibody binding can alter the conformation of antigen and thus influence the k_d (or the avidity of antibody for a specific epitope), only the k_a's were used to assess differences in epitope conformation. Therefore, all subsequent comparisons of the binding of each antibody for the rHDLs were based on the calculated k_a's.

The binding of antibody AI-11 to the large, spherical (CE)-rHDL is shown in Figure 2B. Again, the sensorgrams are shown as a solid line, and the Langmuir model for 1:1 binding that was used to calculate the k_a and k_d rate constants is shown in closed circles. The 12 antibodies listed in Table 1 that had a measurable k_a for plasma HDL were examined for their affinity for each of the rHDL preparations. The observed k_a's for all 12 of these antibodies for the original large, spherical, (CE)rHDL are shown in Figure 5A (solid bars) and ranged from 5970 ± 424 to 142 000 ± 22 600 M^{-1} s^{-1} for antibodies AI-141.1 and AI-187.1, respectively. Importantly, the standard deviations shown in this figure represent the mean of k_a's that were always calculated from separate experiments performed on separate days and confirmed that there was minimal interassay variation.

Effect of rHDL Size on Apo A-I Epitope Expression. The reduction in particle size that occurred when the large, spherical (CE)rHDL were incubated with CETP alone changed the conformation of four apo A-I epitopes (Figure 5A). All four antibodies, AI-115.1, AI-119.8, AI-137.1, and AI-141.1, had a reduced affinity for the small spherical (CE)-rHDL generated by incubation with CETP compared with the large, spherical (CE)rHDL that were incubated with TBS. Interestingly, all of these antibodies bind to apo A-I epitopes that are located in the central region of the molecule spanning residues 115−164 (Figure 1). Antibodies AI-1.2, AI-18, and AI-11, which bind epitopes in the N-terminal one-third of apo A-I, had the same affinity for both the large spherical (CE)rHDL and the small spherical (CE)rHDL. This was also the case for antibodies that bound to the C-terminal portion of apo A-I including antibodies AI-178.1, AI-187.1, and AI-144.7 (Figure 5A). These results suggested that the central region of apo A-I exhibits flexibility when large spherical (CE)rHDL are converted to smaller particles.

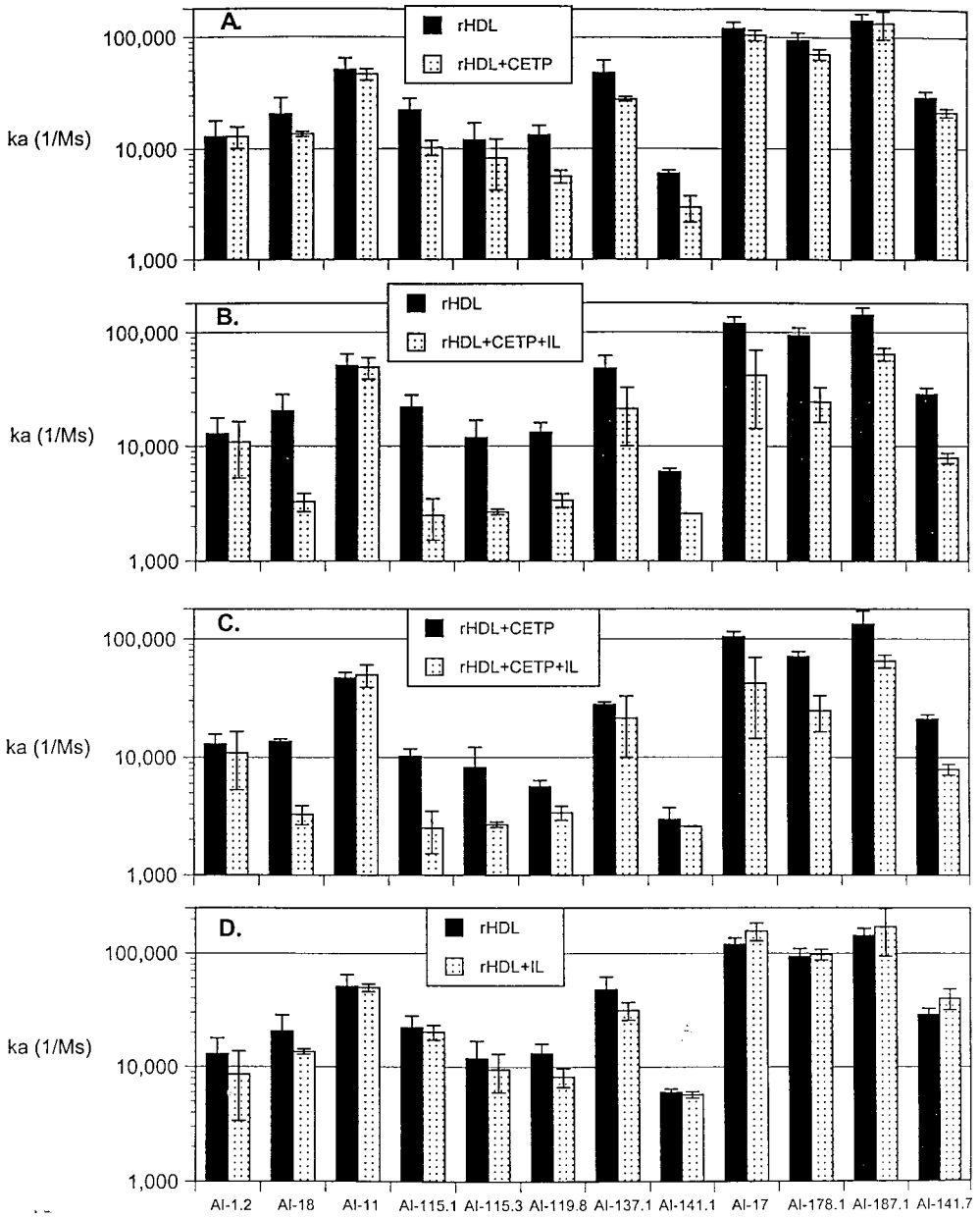

FIGURE 5: Binding of apo A-I-specific monoclonal antibodies to spherical rHDL. All data shown are the calculated association rate constant (k_a) ± SD for each antibody. Multiple concentrations of the same rHDL preparations were always run on at least 2 different days, and separate k_a's for each day were determined. The standard deviations represent this interassay variation. Panel A illustrates the effects of a change from a large to a smaller cholesteryl ester-containing rHDL. The effects of a change from a large CE-enriched particle to a small TG-enriched particle are compared in panel B. Comparison of a small CE-rich particle and a small TG-enriched particle is shown in panel C. Finally, the control rHDL that were incubated either with TBS alone or with TBS and Intralipid in the absence of CETP are compared in panel D.

Effect of rHDL Core Lipid Composition on Apo A-I Epitope Expression. Because rHDL particle size had a limited effect on apo A-I epitope expression, we were surprised to find that, with the exception of 2 N-terminal antibodies, AI-1.2 and AI-11, a decrease in rHDL size and substitution of the core cholesteryl esters with triglyceride significantly decreased the affinity for apo A-I of the 10 other antibodies that were studied (Figure 5B). This result indicated that many domains of apo A-I, including the domains contained within the less flexible α-helices, the β-turns, and the lipophilic C-terminal domain, were altered when large spherical (CE)rHDL were converted into small, spherical (TG)rHDL (Figure 5B).

The effect of rHDL core lipid composition on the conformation of apo A-I was assessed by comparing the binding affinities of the antibodies for the small, spherical (CE)rHDL [generated by incubation of large spherical (CE)-rHDL with CETP] with the small, spherical (TG)rHDL [generated by incubation of large spherical (CE)rHDL with CETP and Intralipid] (Figure 5C). As these rHDL were comparable in size and were both spherical, the data gave direct insight as to how the core lipid composition of HDL affected the conformation of apo A-I. These results showed a significant reduction in the binding affinities for small, spherical (TG)rHDL for 8 of the 12 antibodies tested (Figure 5C).

Table 3: Pairwise Antibody Binding to rHDL

		association rate constant, k_a ($\times 10^5$ M^{-1} s^{-1})			
capture antibody	competing antibody	rHDL	rHDL+CETP	rHDL+CETP+IL	rHDL+IL
AI-17	AI-137.1	nb[a]	nb	nb	nb
AI-137.1	AI-17	0.082[b]	0.15	0.11	0.12
AI-17	AI-178.1	2.22	2.26	2.36	2.18
AI-141.7	AI-178.1	1.62	1.57	1.45	1.44

[a] nb, no binding (i.e., capture and subsequent saturation by antibody AI-17 completely blocked the binding of excess AI-137.1 to all rHDL). [b] In contrast, capture by AI-137.1 did not block the binding of AI-17 to each of the rHDL.

As pointed out earlier, there were some differences in the way the small, spherical (CE)rHDL and the small, spherical (TG)rHDL were prepared. The small, spherical (TG)rHDL that were incubated with CETP and Intralipid had been subjected to three ultracentrifugal spins, whereas the small, spherical (CE)rHDL that were incubated with CETP alone were subjected to two ultracentrifugal spins. This potentially could lead to differences in the physical characteristics of these preparations. To confirm that the differences in binding affinities we observed for the small rHDL were not an artifact of the preparation and isolation procedures, a control rHDL was included in all our SPR analyses. The control rHDL were incubated with TBS alone or with TBS and Intralipid and were not exposed to CETP. The control rHDL were ultracentrifuged using conditions identical to those used for the samples which were incubated with CETP. Importantly, the k_a's for all 12 antibodies were comparable for both of these control rHDL (Figure 5D). These results provided strong evidence that the differences in k_a's shown in Figure 5A−C were reproducible, were due to changes in apo A-I conformation, and were not caused by the preparation, isolation, shipping, and handling procedures.

Pairwise Antibody Binding Analyses. An apo A-I epitope is a spacial entity that is defined by the binding characteristics of a single monoclonal antibody. The size of the surface epitope map on apo A-I defined by any one antibody is limited to the area covered by a single antigen/antibody binding site. To increase the apo A-I surface area on rHDL that could be compared, we examined the binding of pairs of apo A-I antibodies. These antibody pairs were chosen on the basis of (i) the avidity of the first or capturing antibody (only antibodies of good avidity were useful), (ii) the affinity of the second antibody (only antibodies of high affinity were useful), and (iii) the spacial relationship between the two antibody epitopes on a linear representation of apo A-I as illustrated in Figure 1.

The first antibody pair we examined was AI-17 and AI-137.1. These two antibodies bind overlapping epitopes that include residues 143−165 and 137−147, respectively (Figure 1). When each of the rHDL were captured by immobilized AI-17 and subsequently exposed to excess free AI-17 to further saturate all AI-17 epitopes on the captured rHDL, the binding of antibody AI-137.1 was completely blocked (Table 3). This confirmed that these two epitopes remain overlapping on both large and small rHDL and on rHDL that contain either cholesteryl esters or triglycerides in their core. The reverse experiment, the effect of capture and saturation of rHDL by AI-137.1 on the binding of AI-17, was studied as well (Table 3). Interestingly, antibody AI-17 bound each of the AI 137.1-saturated rHDL. Moreover, the k_a's for rHDL+CETP, rHDL+CETP+IL, and rHDL+IL were indistinguishable, whereas the k_a of AI-17 was significantly less ($p < 0.05$) for the control rHDL. This suggested that the affinity of AI-17 for its epitope was greater on both the larger and triglyceride-enriched rHDL and confirmed that the interaction of this pair of antibodies was distinguishable and was not identical for all rHDL.

We also studied the binding of AI-17 and AI-178.1. In contrast to antibody AI-137.1, the binding of antibody AI-178.1, which identifies an epitope that is separated from the AI-17 epitope by 13 residues on a linear representation of apo A-I between residues 178−200 (Figure 1), was not altered by saturation of all the antibody AI-17 epitopes. Moreover, the calculated association rate constants for each of the four rHDLs did not differ (Table 3). These results indicated that antibodies AI-17 and AI-178.1 bound two separate and distinct epitopes on all spherical rHDL and that the relationship between these adjoining, but nonoverlapping, epitopes on apo A-I remained the same on all rHDL irrespective of size or core lipid composition. This same conclusion was reached when two other C-terminal epitopes were studied. This third antibody pair (AI-178.1 and AI-141.7) defines two epitopes represented by aa residues 178−200 and 220−242 (Figure 1). The calculated association rate constants were very similar for the binding of antibody AI-178.1 to each of the rHDLs containing saturating amounts of antibody AI-141.7 (Table 3).

DISCUSSION

The aim of this study was to determine how specific domains of apo A-I are affected by particle size and core lipid composition and how they are organized on the surface of HDL. Guendouzi et al. examined the effect of hepatic lipase-mediated changes in isolated plasma HDL core composition and size *(24)*, and Bergeron et al. *(25)* reported the effects of size and cholesterol content on apo A-I in reconstituted discoidal lipoproteins using traditional immunoassays. In contrast, we used SPR to monitor the binding of well-characterized, homogeneous preparations of rHDL to a panel of epitope-defined, apo A-I-specific monoclonal antibodies. As apo A-I was the only apolipoprotein in the rHDL, and all of the preparations were homogeneous in size and composition, this study has provided a unique insight into the organization of 12 specific domains of apo A-I on the surface of different forms of spherical rHDL. Moreover, it has provided analyses that could not be achieved with plasma HDL, since it contains numerous populations of particles that vary widely in size, composition, and the conformation of apo A-I.

Our starting preparation of rHDL was a homogeneous population of large, spherical particles with cholesteryl esters in their core and apo A-I as the sole apolipoprotein. When

these large, spherical (CE)rHDL were incubated with CETP, small, spherical (CE)rHDL were formed *(15)*. Small, spherical rHDL, which contained triglycerides in their core, (TG)-rHDL, were prepared by incubating large, spherical (CE)-rHDL with CETP and Intralipid *(7)*. To ensure reproducibility of our analyses and to ensure that the results of the SPR experiments could be attributed unequivocally to changes in size or core lipid composition, two separate control rHDL samples, which were incubated in the absence of CETP, also were studied (Figure 5).

Our results showed clearly that the central region of apo A-I contains several mobile domains whose organization is dependent on rHDL particle size. These areas include the epitopes recognized by antibodies AI-115.3, AI-119.8, AI-137.1, and AI-141.1 (Figure 5A). The epitope for AI-115.3 is located in the proline turn between residues 115 and 126, whereas the other three epitopes are located between residues 119 and 164, and span two of the central α-helices in apo A-I (Figure 1). The decreased affinity of these antibodies for their epitopes in small, spherical (CE)rHDL suggested that residues 119−164 of apo A-I are excluded from the surface of small (CE)rHDL.

The decreased affinity of antibody AI-141.1 for residues 141−164 in small, spherical (CE)rHDL was of particular interest, as it may explain why small HDL are more reactive with LCAT than large HDL. This region of apo A-I is important for LCAT activation *(26−28)*, and our observation of reduced binding of antibody AI-141.1 to its epitope in small spherical (CE)rHDL indicated that residues 141−164 may be excluded from the particle surface. This suggested that the mobility of this region of apo A-I is enhanced and its access to the active site of LCAT may be increased.

Our data showing that the affinity of several antibodies for their epitopes in the central and C-terminal regions of apo A-I was decreased in small, spherical (TG)rHDL relative to small spherical (CE)rHDL suggested that there is reduced penetration of apo A-I into the surface monolayer of (TG)-rHDL (Figure 5C). This raised the intriguing possibility that HDL core lipid composition, as well as particle size, may influence the ability of apo A-I to activate LCAT. The molecular volume of TG is 1.5 times greater than that of CE *(29)*. Thus, a TG molecule that partitions into the surface of rHDL will occupy a greater area than a CE molecule, and may prevent some regions of apo A-I from associating with the surface. This is consistent with the findings of Sparks et al., who showed that the apo A-I in TG-containing rHDL had a decreased stability and α-helical content relative to apo A-I in CE-containing rHDL *(30)*.

The reduced affinity of several of the antibodies for their epitopes in small, spherical (TG)rHDL also may reflect the increased lipid−water interfacial hydration of these particles relative to small, spherical (CE)rHDL (*7, 15*). Lipid−water interfacial hydration regulates the penetration of peptides into lipid bilayers *(31)*. If this is also true for the apo A-I in HDL, the more hydrophobic regions of apo A-I may be less able to penetrate the surface of small, spherical (TG)rHDL. Areas of apo A-I which may be affected include residues 119−165, which are recognized by antibodies AI-119.8 and AI-17, and residues 187−210, where antibody AI-187.1 binds.

Of the 12 antibodies studied, only AI-11 and AI-1.2 had comparable affinities for small, spherical (CE)rHDL and (TG)rHDL. Antibody AI-11 recognizes a continuous linear epitope between residues 96 and 111 *(12, 16)*. Our results showing that the organization of this epitope was not affected by rHDL size or core lipid composition raised the possibility that this epitope is highly conserved, and may be important for the structural and functional integrity of HDL. The results of Frank et al. *(32)*, which indicate that residues 100−121 of apo A-I are important for maintaining the stability of discoidal lipid−protein complexes, support this notion. The additional observation that antibody AI-11 blocks the apo A-I-mediated activation of LCAT *(8)* highlights the importance of this region of apo A-I for plasma HDL function.

Antibody AI-1.2 also had a comparable affinity for all the rHDL preparations. This antibody defines a continuous linear epitope spanning residues 1−19 of apo A-I (Figure 1), which has little α-helical content and is not involved in lipid binding *(33)*. Because the association of apo A-I with lipid is unaffected by the deletion of residues 1−43 *(32)*, the extreme N-terminal region of apo A-I may not be in contact with the HDL surface. This could explain why the binding of AI-1.2 was unaffected by changes in rHDL size and core lipid composition.

Our antibody k_a measurements determined how rHDL size and core lipid composition affected an area of apo A-I that was defined by a single antibody. To increase the rHDL surface area that could be probed, we studied interactions of pairs of antibodies that bound to distinct, proximal, and/or overlapping epitopes on apo A-I. We showed that antibody AI-137.1, which bound a small epitope between residues 137 and 147, was blocked by saturating amounts of antibody AI-17, which bound a larger epitope between residues 143 and 165. We also could clearly demonstrate that the antibody that bound the larger overlapping epitope was only partially blocked by saturating amounts of the smaller epitope antibody. Thus, although changes in affinity with antibody pairs were rare, clearly we were able to study the interactions of two antibodies on rHDL using SPR.

In conclusion, this study has provided a unique insight as to how the organizations of 12 specific regions of apo A-I were influenced by the size and core lipid composition of spherical HDL. The results identified several discrete domains in the central region of apo A-I, where conformation was influenced by core lipid composition and particle size. Whereas the N-terminal region of apo A-I was not altered, the organization of the C-terminal region of apo A-I, by contrast, was affected only by rHDL core lipid composition. Although considerable information as to how core lipid composition and particle size affect the structure of rHDL *(7, 15)* is available, the approach used here has enabled us to define for the first time how different conformational states of apo A-I alter 12 discrete linear epitopes on HDL. Such studies will enable us to determine in future studies the impact of these defined structural changes on HDL function.

ACKNOWLEDGMENT

The help of K. Richards and A. Meyers is gratefully acknowledged.

REFERENCES

1. Brouillette, C. G., and Anantharanaiah, G. M. (1995) *Biochim. Biophys. Acta 1256*, 103−129.
2. Gordon, W., Castelli, W. P., Hjortland, M. C., Kannel, W. B., and Dawber, T. R. (1977) *Am. J. Med. 62*, 707−714.

3. Silverman, D. I., Ginsburg, G. S., and Pasternak, R. C. (1993) *J. Med. 94*, 636−645.
4. Leroy, A., Toohill, K. L. H., Fruchart, J., and Jonas, A. (1993)- *J. Biol. Chem. 268*, 4798−4805.
5. Dobiasova, M., and Frohlich, J. J. (1994) *Clin. Chem. 40*, 1554−1558.
6. Jonas, A., Wald, J. H., Toohill, K. L. H., Krul, E. S., and Kezdy, K. E. (1990) *J. Biol. Chem. 265*, 22123−22129.
7. Rye, K.-A., Hime, N. J., and Barter, P. J. (1995) *J. Biol. Chem. 270*, 189−196.
8. Curtiss, L. K., and Banka, C. L. (1996) *J. Lipid Res. 37*, 884−892.
9. Karlsson, R., Michaelsson, A., and Mattsson, L. (1991) *J. Immunol. Methods 145*, 229−240.
10. Nieba, L., Krebber, A., and Plückthun, A. (1996) *Anal. Biochem. 234*, 155−165.
11. Edwards, P. R., and Leatherbarrow, R. J. (1997) *Anal. Biochem. 246*, 1−6.
12. Banka, C. L., Bonnet, D. J., Black, A. S., Smith, R. S., and Curtiss, L. K. (1991) *J. Biol. Chem. 266*, 23886−23892.
13. Rye, K.-A., Hime, N. J., and Barter, P. J. (1996) *J. Biol. Chem. 271*, 4243−4250.
14. Matz, C. E., and Jonas, A. (1982) *J. Biol. Chem. 257*, 4535−4540.
15. Rye, K.-A., Hime, N. J., and Barter, P. J. (1997) *J. Biol. Chem. 272*, 3953−3960.
16. Curtiss, L. K., and Witztum, J. L. (1983) *J. Clin. Invest. 72*, 1427−1438.
17. Curtiss, L. K., and Edgington, T. S. (1985) *J. Biol. Chem. 260*, 2982−2993.
18. Curtiss, L. K., and Smith, R. S. (1988) *J. Biol. Chem. 263*, 13779−13785.
19. Banka, C. L., Black, A. S., and Curtiss, L. K. (1994) *J. Biol. Chem. 269*, 10288−10297.
20. Sorci-Thomas, M. G., Curtiss, L. K., Parks, J. S., Thomas, M. J., and Kearns, M. W. (1997) *J. Biol. Chem. 272*, 7278−7284.
21. Myszka, D. G. (1997) *Curr. Opin. Biotechnol. 8*, 50−57.
22. Morton, T. A., Myszka, D. G., and Chaiken, I. M. (1995) *Anal. Biochem. 227*, 176−185.
23. Roden, L. D., and Myszka, D. G. (1996) *Biochem. Biophys. Res. Commun. 225*, 1073−1077.
24. Guendouzi, K., Jaspard, B., Barbaras, R., Motta, C., Vieu, C., Marcel, Y., Chap, H., Perret, B., and Collet, X. (1999) *Biochemistry 38*, 2762−2768.
25. Bergeron, J., Frank, P. G., Scales, D., Meng, Q. H., Castro, G., and Marcel, Y. L. (1995) *J. Biol. Chem. 270*, 27429−27438.
26. Meng, Q. H., Calabresi, L., Fruchart, J. C., and Marcel, Y. L. (1993) *J. Biol. Chem. 268*, 16966−16973.
27. Lindholm, E. M., Bielicki, J. K., Curtiss, L. K., Rubin, E. M., and Forte, T. M. (1998) *Biochemistry 37*, 4863−4868.
28. Jonas, A. (1998) *Prog. Lipid Res. 37*, 209−234.
29. Sata, T., Havel, R. J., and Jones, A. L. (1972) *J. Lipid Res. 13*, 757−768.
30. Sparks, D. L., Davidson, W. S., Lund-Katz, S., and Phillips, M. C. (1995) *J. Biol. Chem. 270*, 26910−26917.
31. Jacobs, R. E., and White, S. H. (1999) *Biochemistry 28*, 3421−3427.
32. Frank, P. G., Bergeron, J., Emmanuel, F., Lavigne, J. P., Sparks, D. L., Denefle, P., Rassart, E., and Marcel, Y. L. (1997) *Biochemistry 36*, 1798−1806.
33. Palgunachari, M. N., Mishra, V. K., Lund-Katz, S., Phillips, M. C., Adeyeye, S. O., Alluri, S., Anantharamaiah, G. M., and Segrest, J. P. (1996) *Arterioscler. Thromb. Vasc. Biol. 16*, 328−338.

BI992902M